Transform for analysing indirect recordings of bed movement in a flume. The present work aims at exploring different paths for signal analysis.

Conditions of the experimentation

A hydrophone cell was placed within the flow in the vicinity of the bank, at some distance from the river bed (approx. 0.10 to 0.20m). In first attempts, the hydrophone was manually held by the operator with a rod (Fig. 1a). For later experiments, it was supported by a fixed frame (Fig. 1b, 1c).

Figure 1a. The hydrophone hanging from the end of a rod (Isère River)
Figure 1b. The hydrophone held by a fixed frame (torrent de Saint-Pierre)
Figure 1c. The hydrophone on the frame before immersion. In this experiment, an electromagnetic flow sensor is also used (above). During recordings, the set is oriented upstream.

The hydrophone cell used in the experiments is a non-commercial high sensitivity hydrophone which had previously been developed and used for marine applications (Nicolas *et al.*, 2003). Noise recording is made on a DAT recorder (SONY'S TCD-D8). The typical duration of a recording is 30 seconds, digitised as a 16 bits / 44 100 Hz signal. In later experiments, an artificially generated sound was added on the second track of the recording to allow normalization of the recorded intensity between different samples. The pass-band of the recording system is checked through laboratory experiments and covers the range [320 - 22 000 Hz]. This range is sufficient, as noises treated in this paper are within the range [500 - 15 000 Hz].

A first series of recordings was performed in the Isère River, a piedmont river with a narrow system of levees. The main characteristics of the river and its morphology are described elsewhere (Vautier, 2000; Allain-Jegou, 2002). At Lancey where recordings were made, the river width between levees is 80 m and the slope is S_0=0.001. Bed material consists of elongated pebbles with [d_{16}=20 mm, d_{50}=35 mm, d_{84}=45 mm].

The cross section at Lancey is located 15 km upstream of the well-established hydrological station at Grenoble. At the station, the watershed area is 5720 km² and there are no significant tributaries within 45 km distance upstream of this station. Therefore, it can be considered that typical discharges at the station (presented Table 1) are representative of the whole reach where recordings have been made. Instant discharges were evaluated from measurements at Grenoble gage with a suitable time shift.

Table 1: Characteristic discharges at Grenoble gauging station. Q_2 and Q_{10} are the 2 and 10 year return interval discharges. 95 % confidence interval between brackets. (DIREN Rhône-Alpes – Banque Hydro based on 48 years of measurements)

	mean annual discharge	Q_2	Q_{10}
	m^3s^{-1}	m^3s^{-1}	m^3s^{-1}
day average	180	490 [460;530]	750 [690;860]
instant discharge		590 [560;620]	820 [770;910.]

The first recording was made during a flood on 22/03/2001. The discharge at the time of the recording was 805 m^3s^{-1} and is on the order of magnitude for peak discharge during a ten-year return flood. Intense bedload transport was recognized audibly from the surrounding flow noise. It was composed of clear shocks as well as a more confused bottom noise similar to the one that could be made by a continuous sheet of rolling sediment. Although subjective, ear detection served in this demonstration as the reference for comparison with automatic detection of the presence of bedload transport. Our subsequent efforts were oriented towards an automatic treatment of the signal with various analysis techniques.

Time-frequency analysis for individual shock detection

Figure 2 displays a sample of the recorded wave (noise intensity, I vs. time). In this example, the listener recognized three characteristic shocks during this period. The timing of these shocks is indicated in Figure 2 by vertical arrows. There was minimal change in the signal at these recorded times. Hence the representation by intensity is not very well-suited for shock counting and analysis.

A second representation is built where we define P, the instant power of the signal as P=I2-P0, where I2 is the square value of the average noise intensity during time interval Δt. A good discrimination of shocks requires that time interval Δt be shorter than the characteristic duration of a shock which has been estimated from our recordings to be of the order of 3 10^{-3} s. The choice made was $\Delta t=10^{-3}$ s. P0 is the average value of I2. Hence P is proportional to the noise power recorded by the hydrophone.

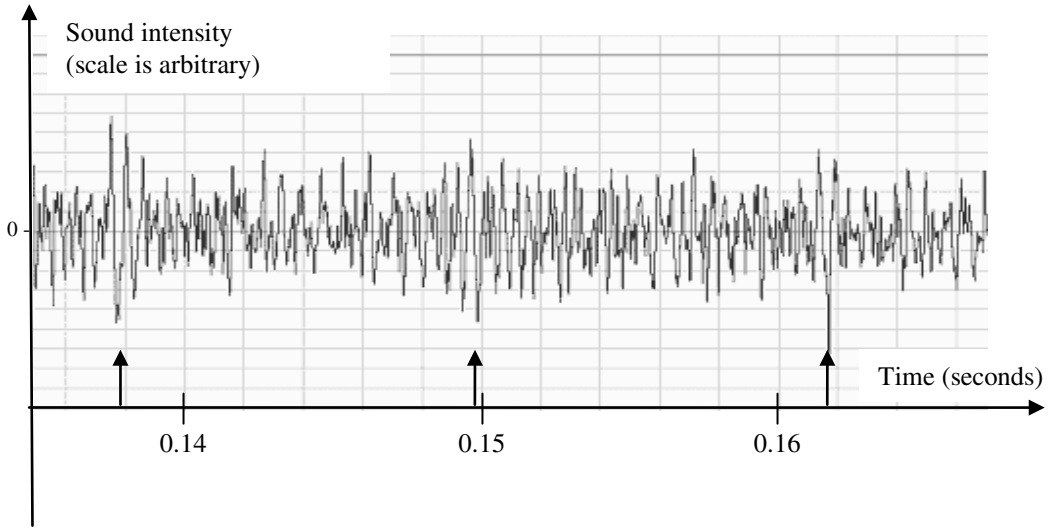

Figure 2. Recorded sound intensity wave from hydrophone. Vertical arrows point to audibly detected shocks which presumably arise due collision with moving bed grains.

A second representation is built where we define P, the instant power of the signal as P=I2-P0, where I2 is the square value of the average noise intensity during time interval Δt. A good discrimination of shocks requires that time interval Δt be shorter than the characteristic duration of a shock which has been estimated from our recordings to be of the order of $3\ 10^{-3}$ s. The choice made was $\Delta t = 10^{-3}$ s. P0 is the average value of I2. Hence P is proportional to the noise power recorded by the hydrophone.

During a shock, sound energy is produced during a very short time interval and the instant power should show a peak value. The same wave sample shown in Figure 2 is represented by the instant power in Figure 3.

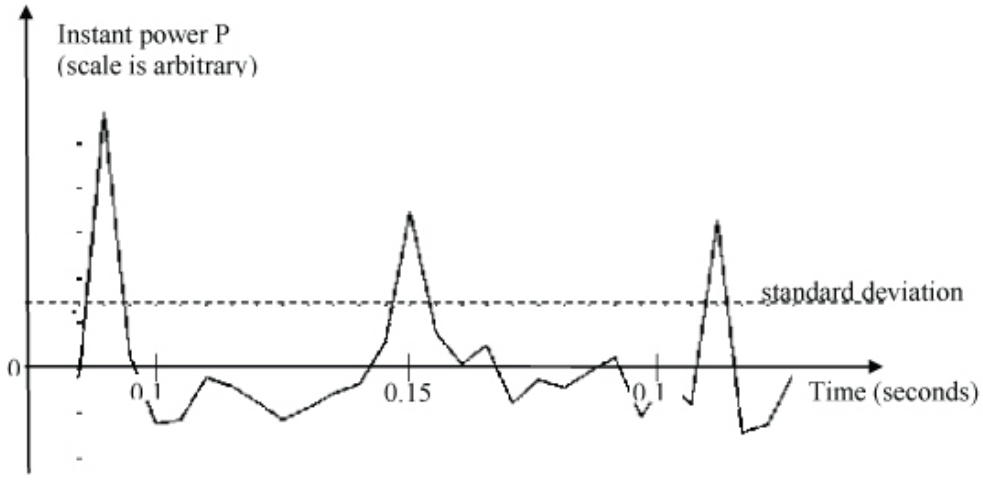

Figure 3. Instant power of recorded sound P=I2-P0 , I2 = square value of the average noise intensity during time interval $\Delta t = 10^{-3}$ s , P0 is the average value of I2. The horizontal dotted line indicates standard deviation.

Instant power displays peak values at the occurrence of shocks as identified audibly, thus confirming the presence of moving grains. However, on other recordings the method does not allow identification of every audibly detected shock. A more refined analysis is required to overcome such a limitation.

The time-frequency analysis (Flandrin, 1998, Flandrin, 1999), or *windowed Fourier transform*, which performs a Fourier transform on limited portions of the original wave signal was applied. In comparison with the basic Fourier transform, the time frequency analysis allows the treatment of non-stationary signals. The time-frequency analysis produces a decomposition of the signal intensity as a function of time and frequency. A typical representation of the analysis is the spectrogram or time-frequency representation (TFR). Figure 4 displays TFR of the same portion of the acoustic signal as in Figure 2 and Figure 3.

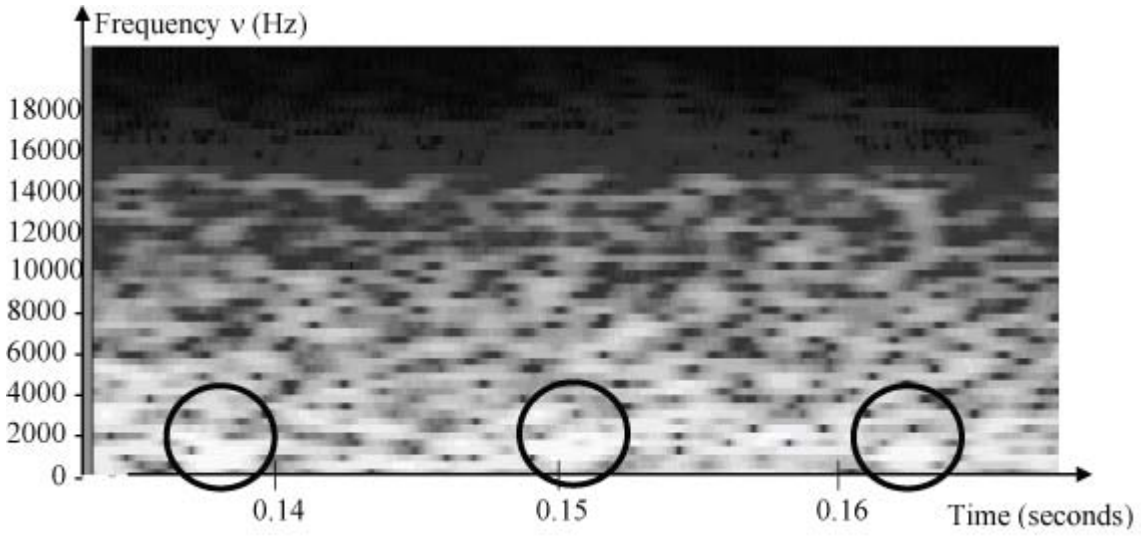

Figure 4. Spectrogram or TFR – A Fourier analysis is performed on discrete portions of the signal (duration Δt). The result appears as rectangular dots (Δt, $\Delta \nu$). The grey scale indicates power spectral density of frequency ν at instant t. Dark areas indicate low sound intensity and clear areas suggest high intensity. Black circles point out to audibly detected signal shocks corresponding to arrows in Fig.2 and peaks in Fig.3. Basic Fourier analysis of the entire recording is displayed in Fig.10 (curve a).

The three shocks which had been previously identified appear as three clear areas on the TFR. For example, the central clear dot between times 0.148 s and 0.152 s shows that a high energy was released with a noise frequency in the interval 1000 - 3000 Hz.

As the calculation of instant power (Fig. 3) took the entire spectral range of the noise into account, this time-frequency analysis permits a similar calculation of the instant power (amount of energy which is released in a given period of time Δt) on discrete frequency ranges [ν, $\nu+\Delta \nu$]. It is then possible to discriminate the instant power produced on a selected range of frequencies. As a consequence of the definition of the Fourier transform, discrimination of frequencies is limited by the size of the time window Δt. A simple expression of this limitation is the Heisenberg-Gabor inequality (a demonstration that can be found in Flandrin, 1998):

$$\Delta t \, \Delta \nu \geq \frac{1}{4\pi} \qquad (1)$$

As a result of the choice $\Delta t = 1\ 10^{-3}$s, the minimal frequency discrimination is $\Delta\nu = 80$ Hz.

Individual shock detection was attempted from filtering instant power $P_{\nu 1,\ \nu 2}$ within the frequency range of audible shocks [$\nu 1$=1000 Hz; $\nu 2$=3000 Hz]. A criterion was devised for the selection of a power peak as characteristic of a shock. After optimization on a sample of the original recording, using audible detection as well as TFR examination, it was determined that a shock is detected only when $P_{\nu 1,\ \nu 2}$ becomes larger than 1.8 times its standard deviation.

This finding is useful because it allows the counting of shocks from a hydrophone recording. Counting has been tested on several samples of the original recording, the average value was 153 shocks per second. The counting of shocks seems to be a suitable method for the investigation of the flux and rhythm of bedload movement. In its present development, it does not allow the quantification of bedload transport because the domain where sediment movement is detected has not been determined.

Another limitation of the method occurs at lower discharges, when bedload transport is less intense and shocks have less energy. Therefore, individual shocks are more difficult to identify by listening or by instant power detection. An example of the hydrophone recordings at the same cross-section on the Isère River (discharge Q=356 m^3s^{-1}, only twice its mean annual value) is shown in Figure 5. Several peaks of instant power value are indicated but discrimination between these minor bedload shocks and other noise of short duration is not possible by listening nor by TFR examination. The energy of bedload shocks is insufficient at such mild flow conditions.

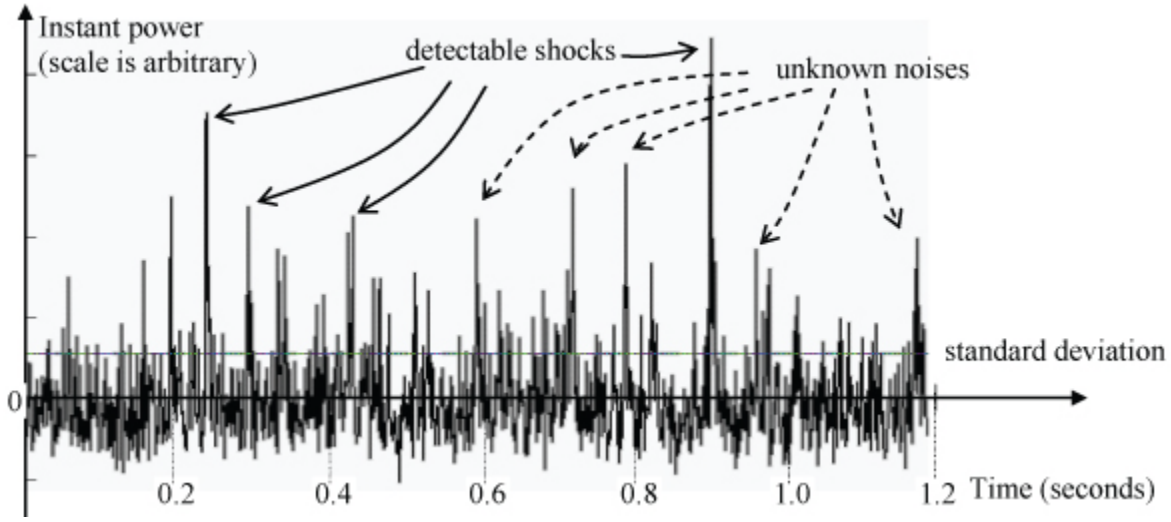

Figure 5. Instant power (356 m^3s^{-1}). For intermediate discharges, shock energy from bed particles shocks is not significantly different from energy from other noises in the same frequency range [1000-3000 Hz]. 'Detectable shocks' are energy peaks identified without doubt by listening.

Grain size and shock noise frequency

An experiment was carried out to determine whether the grain size characteristics of bedload can be identified from our hydrophone recordings. For assessment of the potentials of the method, controlled conditions were preferred in order to minimize uncertainties. The study was conducted in a rectangular basin which had been dug in soil. The cavity shape was a 1m deep cube. It was lined with a plastic cover and filled with water. The bottom was covered with pebbles and same material was poured from underwater onto the bottom. The hydrophone was hung in the centre of the cavity and recorded the

ambient noise of shocks during the pouring. Several runs were made with well sorted and regularly shaped granite pebbles. These are the materials produced by artificial abrasion experiments by Attal, 2003).

From the recordings, samples were selected, each of them corresponding to a single shock/collision, thus artificially increasing shock occurrence and allowing a simple spectral analysis. A graphic representation of the power spectral density (PSD) of one such recording is plotted in Fig. 6, where the dominant frequencies issued by the collision of two pebbles when poured in the basin make a characteristic signature at ca 3300 Hz. The sediment in this experiment had diameters within the range 10 - 20 mm. Two small peaks can be identified on the hump, probably due to some difference in the pebbles involved in this particular shock.

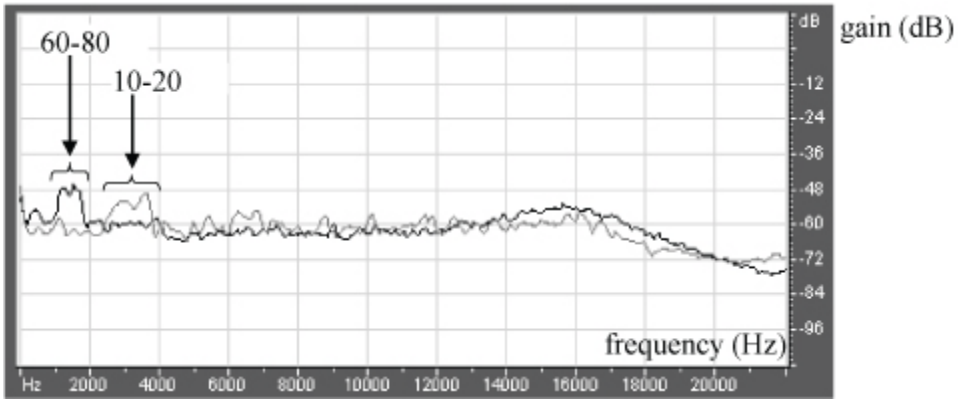

Figure 6. Power spectral densities or PSD from basin experiments (a-grey): 10-20 mm pebbles, (b-black): 60-80 mm pebbles arrows point characteristic chock frequencies

The experiment was repeated with other available collections of the same granite pebbles. Characteristic signatures were identified and the corresponding frequencies were plotted (Fig. 7).

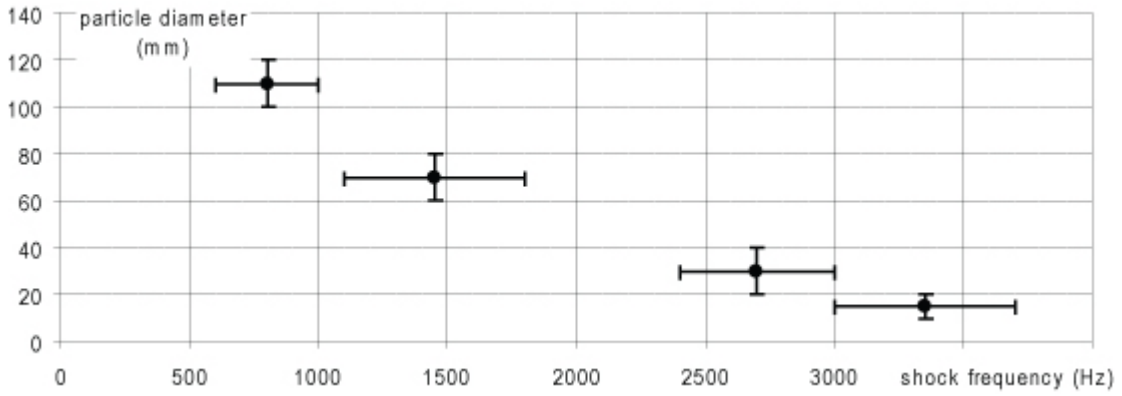

Figure 7. Characteristic frequencies of shocks of individual granite pebbles. Vertical bars indicate the grain size range of each experiment and horizontal bars indicate the characteristic frequency range.

Similar results were obtained by others (e.g. Thorne, 1985, Thorne, 1986, Fouli, 1999). Indeed, dimensional analysis confirms such a proportionality of noise frequency with 1/D. However, the

theoretical value of the frequency of pulsation of a spherical homogeneous solid body (ν in eq. 2, from Dahlen & Tromp, 1998), leads to frequency values about 400 times the measured frequency (ν=456 kHz for d=70mm)

$$\nu = 0.82\pi \frac{C}{r} \tag{2}$$

where C is the celerity of compression waves in the solid (C=6200 m/s in granite) and r is the radius of the sphere. A similar comparison is presented in Thorne (1985) with theoretical vibration frequencies larger by several orders of magnitude than recorded frequencies.

Bed material in real rivers, and especially in the Isère River bed often are flat shaped. Hence, automatic determination of the grain size of transported sediment is more complex; Fouli (1999) has warned of the influence of shape characteristics on noise frequency.

Interpretation

As discussed previously, time-frequency analysis performed on the Isère River recording made during the flood at discharge Q=805 m^3s^{-1} .identified individual shocks the frequency of which has been evaluated in the interval 1000 - 3000 Hz. After filtering and elimination of signal components with a frequency lower than 5000 Hz, we are still able to recognize the shock noise that is characteristic of bedload transport audibly but is not clearly identified by time-frequency analysis.

Our interpretation is that time-frequency analysis, as determined using the described analysis, is only suitable for the detection of the most energetic shocks generated during transport of the coarser sediment (d95=60 mm measured by Vautier, 2000). Finer material is transported as bedload at such flow conditions but with a very high intensity, thus rendering the application of time-frequency analysis unsuitable for the detection of the frequent shocks.

A graphic representation of this interpretation is made on the sketch of Figure 8. The representation uses a Qs (bedload sediment discharge) vs θ relationship, where θ is the dimensionless shear stress, assuming a critical value θc for initiation of transport as in the formulation of Meyer-Peter and Müller (1948). The Qs vs. Δt relationships are sketched for dmin and dmax, the respective the minimum and maximum grain sizes of the bed material.

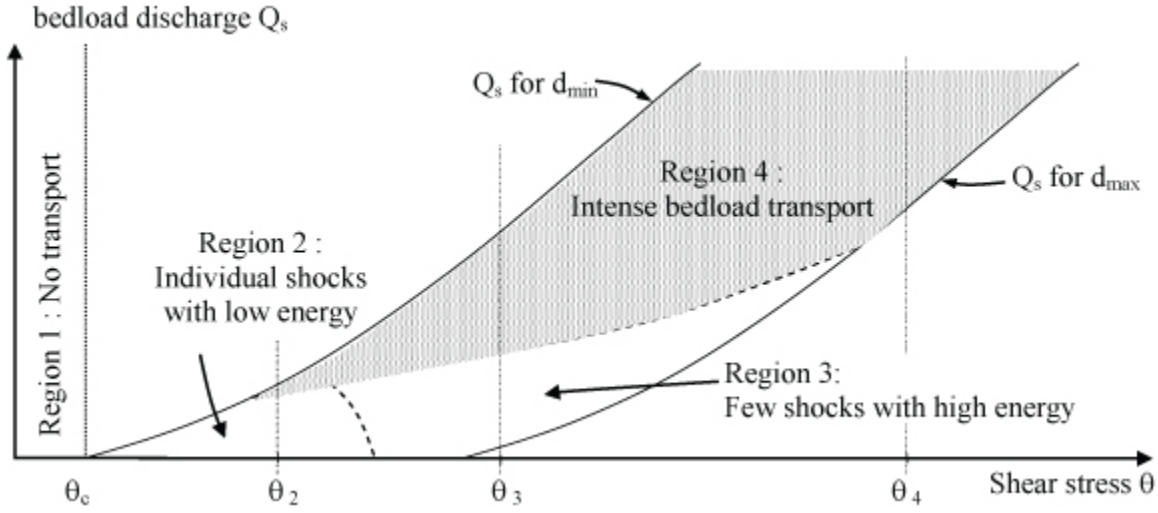

Figure 8. Different regions for shock detection. d_{min} and d_{max} are the extreme grain sizes of bed material; θ_c is the critical shear stress for the onset of transport of the finest particles with d_{min} present on river bed. Q_s is bedload flux.

Several likely progressive regions can be identified on this sketch:

- Region 1: the shear stress is lower than the critical shear for the finest sediment: there is no transport.
- Region 2: for shear stress θ_2, only the finest grain-sized sedimentary particles are transported. Shock energy is low and the discrimination from other noises is difficult
- Region 3: for higher shear stresses θ_3, the coarsest bed material is transported. Corresponding bedload is low but with relative high energy. Corresponding shocks can be discriminated from the surrounding noise by time-frequency analysis.
- Region 4 corresponds to the same shear stress θ_3 but considering finest bed material. For higher stresses it could concern the whole range of bed material. Intense bedload transport and discrimination of individual shocks is not possible by time-frequency analysis.

Region 2 could be identified with Phase I of bedload transport as it was described by Jackson and Beschta (1982). A typical recording was performed at Lancey at a discharge Q=356 m^3s^{-1} (Figure 5) The recording was undertaken at the upstream extremity of a transverse riffle bar. It is assumed that, apart from suspended material, only the finest gravel particles were moving on the coarser, armoured cobble bed of the bar [d_{16}=20 mm, d_{50}=35 mm, d_{84}=45 mm]. It is worth noticing that from Table 1 and station data (DIREN Rhône-Alpes – Banque Hydro), the discharge Q=356 m^3s^{-1} is exceeded on average 20 days a year. Such a discharge is significantly below the discharge with 1.5-year return period which has served for a reference discharge by Ryan *et al.* (2002) for assessing the different phases of bedload transport. For shear stress θ_3, regions 3 and 4 can be identified with Phase II intense bedload transport as described by Jackson and Beschta (1982). The recording at Lancey for Q=805 m^3s^{-1}, nearly the 10-year return period discharge, can be considered as characteristic of Phase II. Its audition presents at the same time the clear energetic shocks from the coarsest particles and a more confused roll from finer particles in movement above the river bed.

Additional spectral analysis

Due to the relative scarcity of shocks in region 3 (Figure 8), the signal from the recording can be considered *non-stationary*. The time-frequency analysis is adapted for such non-stationary signals. The density of shocks is larger in region 4 and the shock noise makes a stationary signal. Therefore, a basic Fourier analysis on the entire recording is adapted and is more convenient as it allows a better discrimination of the different frequencies because the Heisenberg-Gabor inequality is no more a constraint. The purpose of this section is the discrimination on the power spectral distribution of characteristic shock energies from the surrounding flow noise. In what follows, developments are devised from a limited number of experiments. As a result, they lead to hypotheses rather than to real conclusions.

(i) Flow noise spectrum seems to be a constant for a given cross-section

Two recordings were performed at low and medium discharges at the same cross section of the Isere River. The power spectral density (PSD) of each of these two recordings is plotted in Fig. 9.

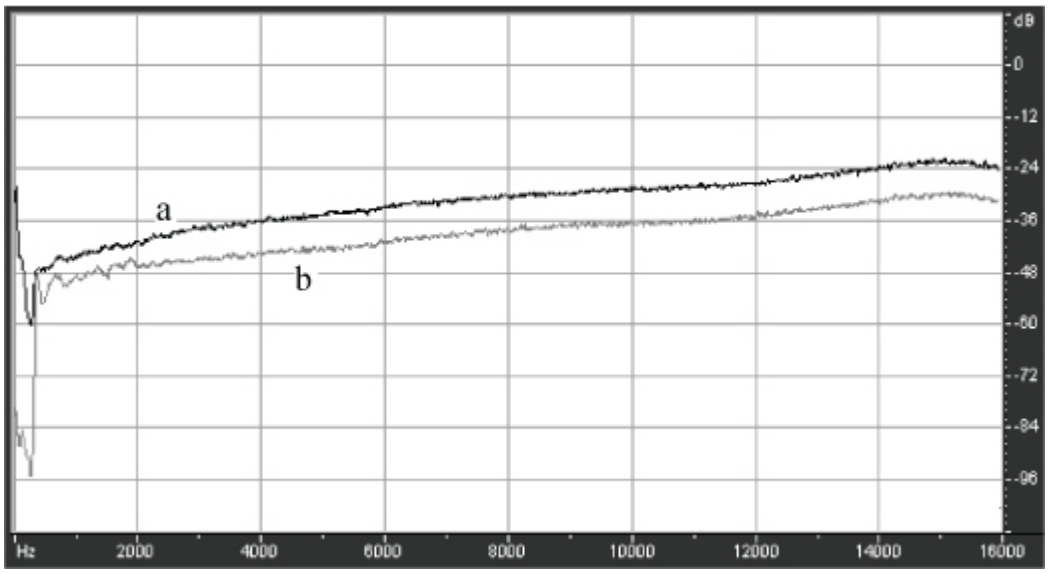

Figure 9. Power spectral densities from Isère Campus section (a-upper curve: 355 m^3s^{-1}; b-lower curve: 217 m^3s^{-1}).

The two recordings show similar spectral characteristics. The PSD representations are nearly parallel curves, with different energies (dB) but with the same frequency distribution. The higher of the two discharges in shown on the upper curve, representing a higher energy level relative to the lower discharge. At low discharge (curve b), the discharge is so low that the recording is from flow noise alone. For medium discharge (curve a), few audible shocks may be recognized by a trained listener but the bed transport is low and likely derives from fine gravel in Region 2 (see Fig. 8). In either case, the spectral signature is mainly issued from flow noise in this cross-section. Such a signature appears to be characteristic of a given cross-section as recordings made at other sections do not have the same frequency distribution.

(ii) A case where bedload noise can be identified from the PSD

Two other PSD representations from a couple of recordings at low and high discharges show the deformation of the curve due to bedload transport (Fig. 10). These were obtained from recordings presented at another cross-section (see Figs. 1-5). The bed material consists of elongated pebbles [d_{16}=20 mm, d_{50}=35 mm, d_{84}=45 mm]. The lower curve plot was obtained with the same recording as in Fig. 5. The discharge (Q=356 m^3s^{-1}) is twice the mean annual value and rare bedload shocks of the gravel produce low energy responses. The upper curve plot was obtained in the same section with the recording made during the decennial flood discharge (Q=805 m^3s^{-1}). The spectral distribution of energy is similar for frequencies in the range 5000 Hz < ν < 15000 Hz (the comparison is limited because the gain of the DAT recorder was not controlled during the recording and the relative position of curves in the vertical direction is uncontrolled). The damping of high frequencies during the flood may be related to high suspended sediment concentrations in such flood conditions. For frequencies ν < 5000 Hz, important bedload transport of the coarsest bed material in flood conditions produces a noticeable increase in energy, visible in Fig.10 by a higher spectral energy on curve (a). Filtering of the signal and elimination of high frequencies in noise recording makes a clearer audition of shocks.

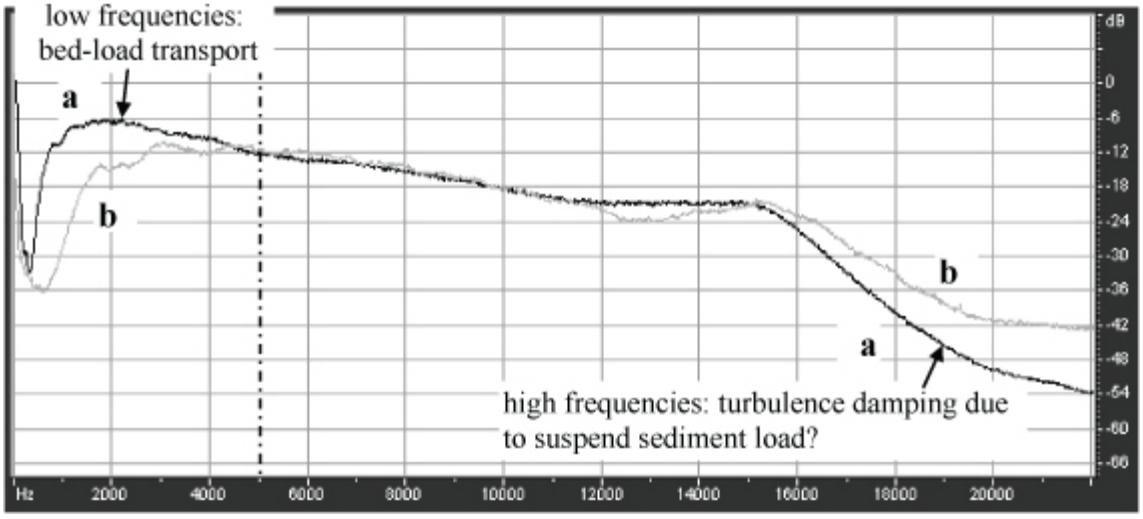

Figure10. Power spectral densities from Isère Lancey section at (a) 805 m^3s^{-1} and (b) 356 m^3s^{-1} .On (a) the deformation of PSD for low frequencies is due to bed-load transport. As the gain is uncontrolled, the relative position of the curves cannot be compared.

In the case of this recording, it can be estimated from the comparison with the PSD representation obtained for the smaller discharge (curve b) that the coarsest moving particles produce energy at about 800 Hz. Because the conditions in the river differ from those in the 'basin experiment', the grain size/frequency relationship presented in Fig. 7 cannot be used to determine the characteristic diameter of the coarsest particles on movement based on signal frequency. When available, this determination of the grain size distribution of bedload using acoustic techniques will be helpful to geomorphologists and engineers in their analysis of the behaviour of gravel beds during floods.

Spectral analysis was also performed on many other recordings. Among them, in many instances shear conditions were likely (schematized) like those of region 2 (Fig. 8), and listening by ear gives no doubt about the occurrence of bedload. Nevertheless, shock energy generated by small particles is low and the number of recorded shocks is insufficient to modify the power spectral distribution which is mainly constructed of noise generated by the moving water (e.g. in Fig. 9).

Conclusions and perspectives

The objective of the paper has been evaluation of the potential of passive sound recording in determining critical conditions for the initiation of bedload transport for different size fractions of the bed material. Different techniques were used for analyzing the signal obtained by *in situ* hydrophone recording of the sound of flow and coarse grain transport.

Calculation of instant power improved our listening-alone ability to identify shocks with high energy. Improved precision was further obtained with time-frequency spectral analysis which allows quantification of shocks generated by intense bedload transport. However, the method is unsuitable where the shock energy is too low or when the shocks are too numerous. Spectral analysis may give a good qualitative estimation of the presence of bedload transport of the coarsest particles within bed-material. Each of these methods may deliver its part of information about the bedload from hydrophone recordings. Further refinements of the methods are needed in determining the flux of bedload from spectral analysis.

Future efforts in this area include:

(i) **Additional data collection.** The exploration and hypotheses presented in this paper are derived from a small number of recordings and were seldom confirmed by repetitive experiments. The priority is collection of a range of recordings in controlled conditions. Artificial floods, as they are produced by the flush of hydroelectric installations (Hauet, 2006, Jodeau, 2007), or the large variations of discharge during a single day in mountain streams (Meunier *et al.*, 2006) are a good opportunity for such experiments.

Bedload transport shocks can be detected, but there is no possibility to determine whether they take place a few centimetres from the hydrophone or in a larger zone. This certainly depends on the one hand on flow conditions and intensity of the turbulence and on the other hand on the sensitivity of the recording system. In mountain streams, whirls, cascades and hydraulic jumps produce very noisy environments and bedload movement is sometimes difficult to detect even with a trained ear. In milder conditions the surrounding noise is less important and the hydrophone used in these experiments has proved to be highly sensitive (e.g. by detection of oars of passing rowing boats more than 50 m away or even the noise of a passing truck on a nearby bridge).

In most of the recordings, the hydrophone was hung in a vertical position by its connecting cable (Fig. 1a). A more stable and controlled position is performed in present recordings (Fig. 1b) but it has not been investigated whether it is a better configuration in terms of sensitivity. The support rod certainly induces significant additional flow noise at frequencies different from those of bedload, but which must be minimized nevertheless. The necessity of additional devices for improving the directivity of noise detection should also be tested, preferably under controlled conditions in a flume.

(ii) **Refine methods**. The authors do not claim to be specialists in signal analysis. The investigations which have been performed are basic and would benefit from additional assessment by those further trained with this method. It is hoped that the investigations have demonstrated the potential of the method. We have identified several limitations and questions which suggest that further refining of the method is needed:

- ☐ Can an efficient filtering eliminate other perturbing noises, or at least improve bedload transport detection?
- ☐ Optimization of time-frequency analysis is needed for a better discrimination of frequencies, and to allow counting in the case of intense transport.
- ☐ Quantification of signal energy: (i) improvement of methods for counting; (ii) could it be related to bedload energy and the velocity of particles, as suggested by Taniguchi *et al.* (1992)?

- Following an idea from Bradeau (1951), location of shocks by correlation of simultaneous recordings of shocks with several hydrophones.

(iii) **Assess sound properties with direct measurement of bedload.** Systematic measurements of bed material properties and velocity will be performed for the next experiments for the assessment of shear conditions in relation to signal properties. A simple installation is shown in Fig. 1c with an electromagnetic flow sensor associated with the hydrophone on the support rod. Ryan et al. (2005) mentioned the difficulty as *"to make progress toward development and validation of surrogate technologies until there is a way to adequately quantify the rates of bedload transport"*. Despite limitations and sometimes low confidence in some of the classical methods, field comparisons are necessary with direct measurement of the bedload such as physical samplers or particle tracking.

Costs

The replacement of the recording system has been estimated at approx. 6000 €.

Acknowledgments

This work is part of the project *Développement méthodologique de la mesure du transport de fond dans les rivières* supported by the programme RELIEFS de la Terre - INSU/CNRS. Acknowledgments to GIP-SA Lab from which the hydrophone used during experiments was borrowed http://www.gipsa-lab.inpg.fr/index.php?id=392. Sincere thanks are given to Sandra E. Ryan, Jonathan B. Laronne and James Bathurst for their fruitful suggestions and their patient correction of the English language.

References cited

Allain-Jégou, C., 2002, Relations végétation-écoulement-transport solide dans le lit des rivières : étude de l'Isère dans le Grésivaudan. *(Relations between vegetation, flow and solid transport river beds)* Unpublished Ph.D. thesis, Institut National Polytechnique de Grenoble, 197 p. (*http://www.lthe.hmg.inpg.fr/~belleudy/Recherche/These_CA.pdf*).

Attal, M., 2003, Erosion des galets des rivières de montagne au cours du transport fluvial : étude expérimentale et application aux réseaux hydrographiques d'orogènes actifs.*(Erosion of cobbles in mountain rivers during bedload transport:experimental study and application to hydrographic systems in active orogenic settings)* . Unpublished Ph.D. thesis, Université Joseph Fourier, Grenoble (*http://tel.archives-ouvertes.fr/tel-00004097/fr/*).

Bänziger, R. and Burch, H., 1990, Acoustic sensors (hydrophones) as indicators for bedload transport in a mountain torrent, in Hydrology in Mountainous Regions, IAHS Publ.193, pp. 207-214.

Barton, J.S., Slingerland, R.L., Pittman, S.and Gabrielson, T.B., 2008. Monitoring coarse bedload transport with passive acoustic instrumentation: A field study. USGS SIR, this volume.

Belleudy, P., 1992, Modeling Danube and Isar Rivers morphological evolution (2nd part): Comparison of field data with modeling results. Proc. of the 5th International Symposium of River Sedimentation, Karlsruhe, Germany, pp. 1208-1216.

Belleudy, P., 2000, Restoring flow capacity in the Loire River bed. Hydrological Processes, v. 14, pp. 2331-2344.

Bogen, J. and Moen, K., 2003, Bedload measurements with a new passive ultrasonic sensor, *in* Erosion and Sediment Transport Measurement: Technological and Methodological Advances, Oslo, IAHS, pp. 181-192.

Bradeau, G., 1951, Quelques techniques pour l'étude et la mesure de débit solide. La Houille Blanche, v.A, 243 p.

Cortier, B. and Couvert, B., 2001, Causes et conséquences du blocage actuel de la dynamique fluviale et du transit sédimentaire du Rhône. La Houille Blanche, v. 56, pp. 72-78.

Couvert, B., Lefort, P., Peiry, J-L. and Belleudy, P., 1999, La gestion des rivières - Transport solide et atterrissements - Guide méthodologique. Les études des Agences de l'Eau, n° 65. ISSN : 1161- 0 4 2 5 (*http://www.km-dev.com/eaufrance/francais/etudes/pdf/etude65.pdf*).

Dahlen, F. A., and Tromp, J., 1998, Theoretical Global Seismology, Princeton University Press, 944 p.

De Linares, M., 2007, Modélisation numérique bidimensionnelle du transport solide et de la dynamique fluviale. Validation sur deux sites en Loire et sur l'Arc. *(Two-dimensional numerical modelling of bed load transport and fluvial morphology. Validation on two sites on the Loire river and on the Arc river).* Unpublished Ph.D. thesis, Université Joseph Fourier, Grenoble (*http://tel.archives-ouvertes.fr/tel-00193119/fr/*).

De Linares, M., Belleudy, P., 2007, Critical shear stress of graded sediment in sand gravel rivers. J. of Hydraulic Engineering-ASCE, pp. 555-559.

Egiazaroff, I. V., 1965, Calculation of nonuniform sediment concentration. J. Hydraul. Div., ASCE , No.HY4 v. 91, pp. 225-247.

Flandrin, P., 1998, Temps-Fréquence: Traité des Nouvelles Technologies, série Traitement du Signal, Hermès, Paris.

Flandrin, P., 1999, Time-frequency/time-scale analysis: Wavelet Analysis and its Applications, v. 10, Academic Press Inc., San Diego, CA, xii+386 p.

Fouli, H., 1999, Acoustic analysis of streams for bedload transport prediction. 28th IAHR Congress.

Froehlich, W., 2003, Monitoring of bedload transport by use of acoustic and magnetic device, *in* Erosion and Sediment Transport Measurement in Rivers—Technological and Methodological Advances, Publication 283, IAHS, pp. 201-210.

Hauet, A., 2006, Estimation de débit et mesure des vitesse en rivière par Large-Scale Particle Image Velocimetry *(Discharge estimation and surface velocity measurement in river using Large-Scale Particle Image Velocimetry).* Unpublished Ph.D. thesis, Institut National Polytechnique de Grenoble, 305 p. (http://tel.archives-ouvertes.fr/tel-00116889/fr/).

Henderson, F. M., 1966, Open channel flow, Macmillan.

Jackson, W. L. and Beschta, R. L., 1982, A model of two-phase bedload transport in an oregon coast range stream. Earth Surface Processes and Landforms, v. 7, pp. 517-527.

Jodeau, M., 2007, Morphodynamique d'un banc de galets en rivière aménagée lors de crues *(Gravel bar morphodynamics in an engineered river during high flow events)*. Unpublished Ph.D. thesis, Université Claude Bernard, Lyon (http://tel.archives-ouvertes.fr/tel-00198125/fr/).

Krein, A., Klinck, H., Eiden, M., Symader, W., Bierl, R., Hoffmann, L., and Pfister, L., 2008, Investigating the transport dynamics and the properties of bedload material with a hydro-acoustic measuring system. Earth Surface Processes and Landforms, v. 33, pp. 152-163.

Labaye, G., 1948, Note sur le débit solide des cours d'eau. La Houille Blanche, v. A, pp. 3-30.

Meunier, P., Metivier, F., Lajeunesse, E., Meriaux, A. S. and Faure, J. 2006, Flow pattern and sediment transport in a braided river: The "torrent de St Pierre" (French Alps). Journal of Hydrology, v. 330, pp. 496-505.

Meyer-Peter, E. and Müller, R., 1948, Formulas for bed-load transport. 2nd Meeting, Intl. Ass. Hydraul. Structures Res., pp. 39-64.

Mizuyama, T., Fujita, M. and Nonaka M., 2001, Measurement of bedload with the use of hydrophone in mountain torrents, *in* Erosion and Sediment Transport Measurement in Rivers—Technological and Methodological Advances, Publication 283, IAHS, pp. 222-227

Muhlhofer, L., 1933, Untersuchung uber die schwebestoff- und geschiebefuhrung des Inn nächst Kirchbichl.. Die Wasserwirtschaft, Nos. 1-6.

Nicolas, B., Mars, J.I. and Lacoume, J-L., 2003, Geoacoustical parameters estimation with impulsive and boat noise source. IEEE Journal of Oceanic Engineering, v. 28, pp. 494-501.

Parker, G., 1978a, Self formed rivers with stable banks and mobile bed: Part I, the sand silt river. Journal of Fluid Mechanics, v. 89, pp. 109-126.

Parker, G., 1978b, Self formed rivers with stable banks and mobile bed: Part II, the gravel river. Journal of Fluid Mechanics, v. 89, pp. 127-148.

Rickenmann, D., 1997, Sediment transport in Swiss torrents. Earth Surface Processes and Landforms, v. 22, pp. 937-951.

Ryan, S. E., Bunte, K. and Potyondy, J. P., 2005, Breakout Session II: Bedload Transport Measurement, Data Uncertainties and New Technologies. Federal intergagency sediment monitoring instrument and anaysis research workshop, pp. 16-28.

Ryan, S. E., Porth, L. S. and Troendle, C. A., 2002, Defining phases of bedload transport using piecewise regression. Earth Surface Processes and Landforms, v. 27, pp. 971-990.

Taniguchi, S., Itakura, Y., Miyamoto, K. and Kurihara, J., 1992, A new acoustic sensor for sediment discharge measurement, *in* Erosion and sediment transport monitoring in river basins, v. 210, IAHS, pp. 135-142.

Thorne, P. D., 1985, The measurement of acoustic noise generated by moving artificial sediments. Journal of the Acoustic Society of America, v. 78, pp. 1013-1023.

Thorne, P. D., 1986, Laboratory and marine measurements on the acoustic detection of sediment transport. Journal of the Acoustic Society of America, v. 80, pp. 899-910.

VanRijn, L. C., 1984, Sediment transport. Part I: bedload transport. J. Hydraul. Eng., v. 110, pp. 1431–1456.

Vautier, F., 2000, Dynamique géomorphologique et végétalisation des cours d'eau endigués: l'exemple de l'Isère dans le Grésivaudan *(Morphological dynamic and vegetation growth in embankedrivers)*. Unpublished Ph.D. thesis, Université Joseph Fourier - Grenoble.

Wilcock, P. R. and Crowe, J. C., 2003, Surface-Based Transport Model for Mixed-Size Sediment. J. Hydraul. Eng., v. 129, pp. 120-128.

Wolman, M. G. and Miller, J. P. 1960, Magnitude and frequency of forces in geomorphic processes. Journal of Geology, v. 68, pp. 54–74.